Int. J. Electrochem. Sci., 16**(2021)** Article Number: 211137, doi: 10.20964/2021.11.33

International Journal of ELECTROCHEMICAL SCIENCE
www.electrochemsci.org

Synthesis of NiO-CNTs nanocomposite for modification of glassy carbon electrode and Application for Electrochemical determination of fentanyl as an opioid analgesic drug

Hao Ding, Wei Tao[*]

Foundation Course Department, Wenhua College, Wuhan, 430074, China
[*]E-mail: tweiwhu@163.com

Received: 23 July 2021/ *Accepted:* 13 September 2021 / *Published:* 10 October 2021

This study was focused on the synthesis of nanocomposite based on NiO and CNTs (NiO@CNTs) for modification of glassy carbon electrode (GCE) and application for electrochemical determination of fentanyl as an opioid analgesic drug. The NiO@CNTs nanocomposite was electrodeposited on the GCE surface. Results of structural analyses using SEM and XRD showed that the surface of the 3D of CNTs network was homogeneously covered by NiO nanoparticles, and the simultaneous electrodeposition of NiO nanoparticles and functionalized CNTs on GCE had been created a core-shell structure of NiO and CNTs with large void space between neighboring nanostructures. The results of electrochemical studies using CV and DPV techniques exhibited that the good conductivity of NiO and CNTs can contribute to the enhancement of the electrochemical response of the electrode toward fentanyl. The NiO@CNTs/GCE showed the selective and stable to determination fentanyl, and sensitivity, the limit of detection and linear range of NiO@CNTs/GCE as fentanyl sensor were obtained 1.12219 μA/μM, 0.01 μM and 10 to 160 μM, respectively. Moreover, a comparison between the obtained sensing results of NiO@CNTs/GCE with reported fentanyl electrochemical sensor demonstrated comparable or better sensing properties and a wider linear range of NiO@CNTs/GCE than other reported electrochemical sensors. The results of the study indicated that the performance and precision of prepared electrodes for the analysis of fentanyl pharmaceutical and human serum samples showed acceptable precisions with appropriate recovery and RSD values. Therefore, of NiO@CNTs/GCE can be applied to accurate and reliable determination of fentanyl in clinical analyses.

Keywords: NiO@CNTs nanocomposite; Fentanyl; Clinical Samples; Differential pulse voltammetry; Selectivity

1. INTRODUCTION

Fentanyl (*N*-phenyl-*N*-[1-(2-phenylmethyl)piperidin-4-yl]propanamide) as an agonist of μ-opioid receptors is a powerful synthetic, lipophilic phenylpiperidine opioid that is similar to morphine but is 50 to 100 times more potent [1, 2]. In general, selectively bond of opioid receptors of fentanyl to

μ-opioid receptor outside the central nervous system leads to activation of the mu-subtype opioid receptor and results in hyperpolarization and reduced neuronal excitability [3, 4]. Like morphine, prescription fentanyl is typically used to treat patients with severe or to manage pain after surgery pain during or after an operation [5, 6]. This prescription drug is also sometimes drugs are manufactured illegally, and sold on the street and used like other illegal drugs [7, 8].

Fentanyl sometimes shows side effects such as drowsiness, nausea, constipation, low blood pressure, problems breathing and unconsciousness [9, 10]. Moreover, it is highly addictive and Additional psychological signs of fentanyl abuse include confusion, impaired judgment, disorientation, anxiety, depression, paranoia, rapid mood swings, depression, coma and hallucinations [11, 12]. Therefore, distinguish and detect the level of fentanyl as more dangerous drug than heroin is necessary to prevent abuse, an epidemic of addictive disorders and protect crime [13, 14]. Accordingly, many types of research have been conducted on the determination of the fentanyl level in pharmaceutical species and bodily fluids such as urine and blood using chromatography, radioimmunoassay, colorimetry, surface-enhanced Raman spectroscopy, mass spectrometry, ultraviolet detection and electrochemistry [15, 16].

Between these methods, there is currently significant interest in electrochemical techniques for the cheaper, faster and safer analysis of inorganic and organic analytes [17-20]. Moreover, the modification of the electrode surface using nanostructures and composites has been promoted the sensitivity and selectivity of electrochemical sensors. Therefore, this study was focused on the synthesis of nanocomposite based on NiO and CNTs for modification of glassy carbon electrode and application for electrochemical determination of fentanyl as an opioid analgesic drug.

2. MATERIALS AND METHOD

2.1. Synthesis nanocomposite of NiO@CNTs

1 g CNTs (99%, Guangzhou Hongwu Material Technology Co., Ltd., China) with an average length of 1-2μm and an average outer diameter of 10-30nm were ultrasonically functionalized in 100 mL of 3:1 H_2SO_4 (50%, Sigma-Aldrich) and HNO_3 (60%, Sigma-Aldrich) for 50 minutes at 45°C[21]. The obtained black solid was filtered using a 0.22 μm membrane filter (Millipore, Hangzhou Tianshan Precision Filter Material Co., Ltd., China) and washed with deionized water several times, and then dried at 80°C under vacuum for 10 hours. The functionalized CNTs were ultrasonically dispersed in a 0.07 wt% Triton X-100 (Merck, Germany) solution for 3 hours. Next, the obtained suspension was filtered and washed repeatedly with deionized water and dried at 30°C under vacuum for 12 hours. Subsequently, 300 mg of product was sonicated in 70 mL of 0.1 M $NiCl_2$ (≥98%, Sigma-Aldrich) solution for 60 minutes. The prepared suspension was used as an electrodeposition electrolyte.

Prior to electrodeposition, the glassy carbon electrode (GCE) surface was polished with alumina slurry (96%, 0.3 and 0.05 μm, Chengdu Huarui Industrial Co., Ltd., China) and thoroughly washed in ethanol (99%, Shandong Aojin Chemical Technology Co., Ltd., China) and deionized water for several times, respectively. Afterward, the GCE was used as the working electrode in the

electdeposition cell which contained two other electrodes; Ag/AgCl (KCl 3M) as the reference electrode and Pt wire as the counter electrode. Electrodeposition was performed in Autolabpotentiostat/galvanostat (PGSTAT30, Eco Chemie, Utrecht, Netherlands) at the potential range of -1.2 V to +1.2 Vat scan rate of 50mV/s during 20 minutes. NiO@CNTs/GCE was used as a working electrode for electrochemical studies.

2.2. Real samples preparation

Real samples in this study were prepared from pharmaceutical and biological samples. Fentanyl (Effentora, Teva Canada Innovation) 100 µg buccal tablets were provided as a pharmaceutical sample that each tablet contains 100µg fentanyl. For the preparation of the 1mg/ml fentanyl solution of Effector tablets, 10 tablets were dissolved in 100 ml of 0.1 M phosphate buffer solution (PBS). In order to prepare the real sample from human serum, the Fentanyl-free serum sample was provided from Beijing Cancer Hospital (Beijing, China). 10mL of serum samples were diluted to 100mL with the 0.1 M PBS. DPV measurement in 0.1M PBS pH 7.0 at a scan rate of 20mV/s with the standard addition method applied to analytical studies of real samples.

2.3. Characterization

Cyclic voltammetry (CV) and differential pulse voltammetry (DPV) analyses were also conducted on Autolabpotentiostat/galvanostat system using three electrode-electrochemical cell containing working electrode (bare GCE or modified GCE), and counter electrode (Pt wire) and reference electrode (Ag/AgCl (KCl 3M) in 0.1 M PBS pH 7.0 as electrochemical electrolyte which prepared from equal volume ratio of 0.1 M NaH_2PO_4 (99%, Merck, Germany) and 0.1 M Na_2HPO_4 (≥99.0%, Sigma-Aldrich). Scanning electron microscopy (SEM, JSM-5510LV, JEOL Ltd., Tokyo, Japan) and X-ray diffractometer (XRD, Phillips PW1800) were used to study the morphological and structural properties of modified electrodes.

3. RESULTS AND DISCUSSION

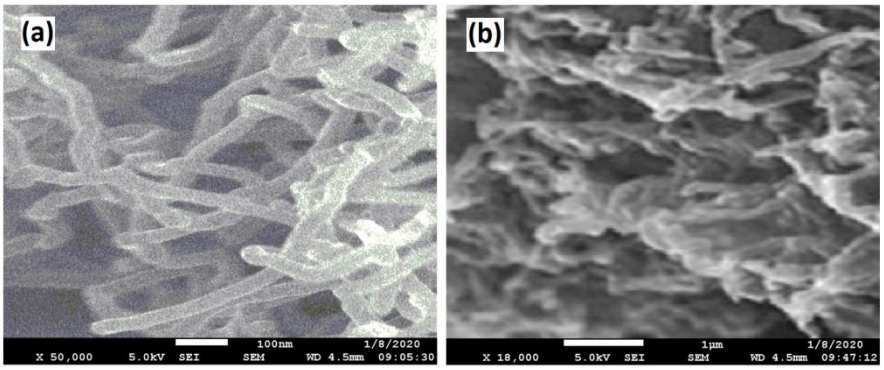

Figure 1. SEM images (a) CNTs/GCE, (b) NiO@CNTs/GCE.

Figure 1 shows the SEM images CNTs/GCE, NiO/GCE and NiO@CNTs/GCE. As observed from Figure 1a, the CNTs were coaxially and uniformly electrodeposited on GCE with an average length of 1 µm and an average outer diameter of 30 nm. 3D of CNTs architecture was contained of interconnected nanotubes. The high surface-to-volume ratio and functionalized groups on edge and surface of CNTs make them useful substrates for the uniform decoration of metallic nanoparticles [22]. Figure 2b depicts the morphology of NiO@CNTs/GCE which reveals that the surface of the 3D of CNTs network is homogeneously covered by NiO nanoparticles. The functionalized group on CNTs surface facilitate the interaction between the metal ions and CNTs in electrodeposition process which formed metal adsorbed on the CNTs surface [23]. Simultaneous electrodeposition of NiO nanoparticles and functionalized CNTs on GCE has been created a core-shell structure of NiO and CNTs with large void space between neighboring nanostructures which can be beneficial for fast charge transfer in electrochemical reactions and easy access of electrolyte ions [24]. The average diameter of the core-shell structure of NiO@CNTs is 30 nm.

Figure 2 shows the XRD patterns of powders of CNTs, NiO and NiO@CNTs. As observed from Figure 2a, there are two diffraction peaks at 26.15° and 43.22° for the X-ray diffraction pattern of CNTs which related to (002) and (100) graphitic planes, respectively (JCPDS card no. 75-1621) [25]. The XRD pattern of NiO in Figure 2b shows the diffraction peaks at 37.21°, 43.31° and 62.88° which attributed to the formation the (111), (200) and (220) planes of cubic NiO (JCPDS card no. 43-1477). The XRD pattern of NiO@CNTs in Figure 2c also shows the diffraction peaks of (111), (200) and (220) of NiO and additional peaks (002) of CNTs which indicated to successfully electrodeposition of NiO nanoparticles onto the CNTs, and in agreement with the SEM results.

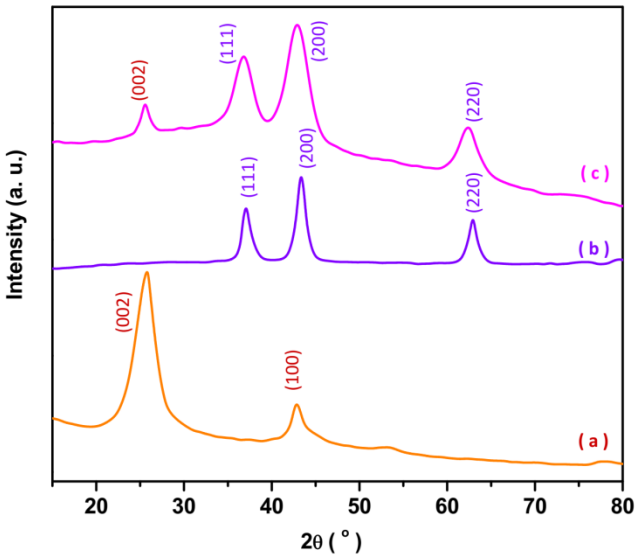

Figure 2. XRD patterns of powders of (a) CNTs, (b) NiO and (c) NiO@CNTs.

In order to investigation the electrochemical properties of bare GCE and modified GCE, the CV measurements were performed in 0.5 M KOH at a scan rate of 20 mV/s. Figure 3 shows the CV curves of GCE, CNTs/GCE, NiO/GCE and NiO@CNTs/GCE. As seen from Figures 3a and 3b, there are no redox peaks for the CV curves of the GCE and CNTs/GCE, and CV curves of the CNTs/GCE

show a larger CV integral area which indicted to more active sites and enhanced surface area [26, 27]. the CV curves of NiO/GCE and NiO@CNTs/GCE in Figures 3c and 3d show redox peaks which attributed to more electroactivity of metal ions and redox mechanism as following reversible reaction [28]:

$$NiO + OH^- \leftrightarrow NiOOH + e^- \qquad (1)$$

Furthermore, the NiO@CNTs/GCE electrode shows stronger reduction and oxidation peaks and a larger integral area than NiO/GCE and CNTs/GCE that it associated with a larger active surface area of the electrode and faster charge transport [29]. Moreover, it was reported that CNT decorated with Ni varies from well-organized clusters to complete coverage of the surface resulting in electronic charge transfer and formation of Ni-C bond [30].

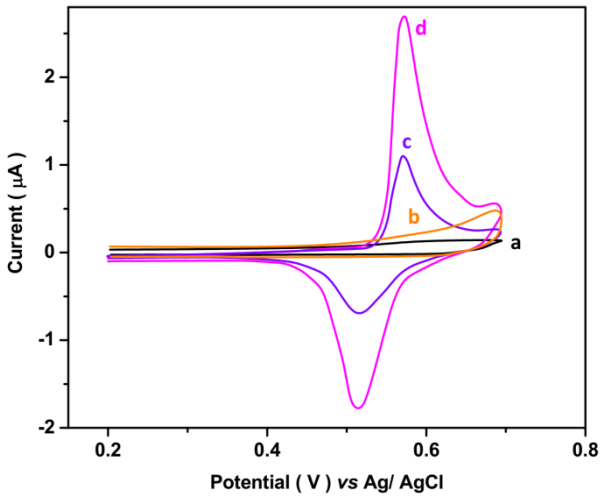

Figure 3. CV curves of GCE, CNTs/GCE, NiO/GCE and NiO@CNTs/GCE in 0.5 M KOH at a scan rate of 20 mV/s.

Figure 4 shows the electrochemical response of electrodes to the presence of 10μM fentanyl in 0.1M PBS pH 7.0at a scan rate of 20 mV/s. it can be observed that the CV curves of GCE, CNTs/GCE, NiO/GCE and NiO@CNTs/GCE demonstrates the electrochemical response toward fentanyl at the potential of 0.70, 0.62, 0.62 and 0.64 V, respectively which corresponded to oxidation of fentanyl[15, 31]. The CV curve of NiO@CNTs/GCE shows the high electrochemical response that is correlated to faster electron transfer between NiO@CNTs and electrolyte [32]. Additionally, the high surface area, and the mesopores structure of NiO@CNTs can facilitate the ion diffusion between electrode and electrolyte [33, 34]. The good conductivity of NiO and CNTs can contribute to the enhancement of the electrochemical response of the electrode. Therefore, the NiO@CNTs/GCE was used for further electrochemical studies.

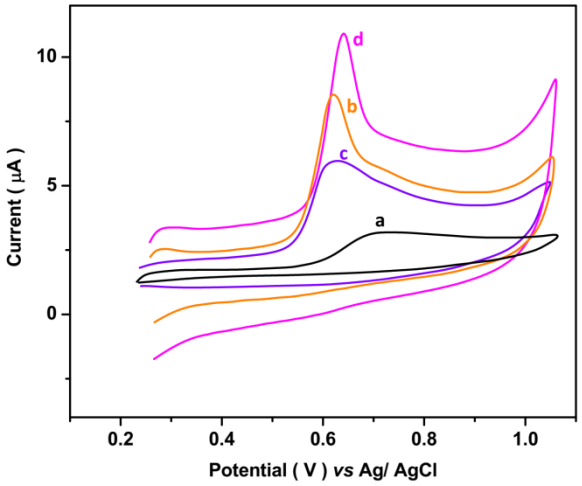

Figure 4.CV curves of (a) GCE, (b) CNTs/GCE, (c) NiO/GCE and (d) NiO@CNTs/GCE in presence of 10µM fentanyl in 0.1M PBS pH 7.0 at a scan rate of 20 mV/s.

The stability of response of NiO@CNTs/GCE toward fentanyl was investigated under successive CV. Figure 5 shows the first and 50th recorded CV curves of electrochemical response of NiO@CNTs/GCE in presence of 10µM fentanyl in 0.1M PBS pH 7.0at a scan rate of 20 mV/s that it is illustrated to 4% decrease of peak current, indicating to high stability response of NiO@CNTs/GCE for determination of fentanyl because of covalent and non-covalent binding of NiO nanoparticles to the carboxylic group of functionalized CNTs [35]. In addition, the high mechanical and chemical stability of NiO nanoparticles and CNTs significantly promotes the stability of electrochemical response of NiO@CNTs/GCE.

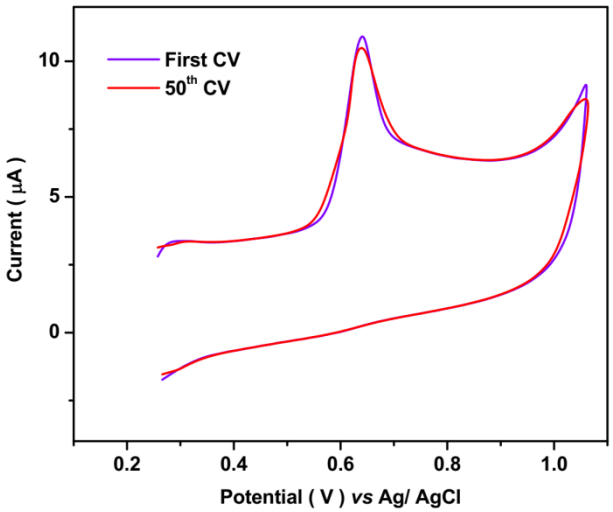

Figure 5. (a) First and (b) 50th recorded CVs curves of electrochemical response of NiO@CNTs/GCE in presence of 10µM fentanyl in 0.1M PBS pH 7.0at a scan rate of 20mV/s.

Figure 6a displays the DPV curves of NiO@CNTs/GCE for successive injections of 10µM fentanyl in 0.1M PBS pH 7.1at a scan rate of 20mV/s. it is observed as the fentanyl content increases, the oxidation peak current also increases linearly. The resulted calibration plot in Figure 6b reveals that the sensitivity and limit of detection of NiO@CNTs/GCE to the determination of fentanyl are obtained 1.12219µA/µM and 0.01µM, respectively. Further electrochemical experiments to evaluate the linear range of NiO@CNTs/GCE toward fentanyl were carried out in successive injections of 20 µM fentanyl solution in electrochemical cell. Figures 7 exhibits the resulted calibration plot which presented the linear range for the determination of fentanyl on NiO@CNTs/GCE is 10 to 160µM. The departure from linearity is observed for a further injection of fentanyl because of saturation of the active sites of the electrode.

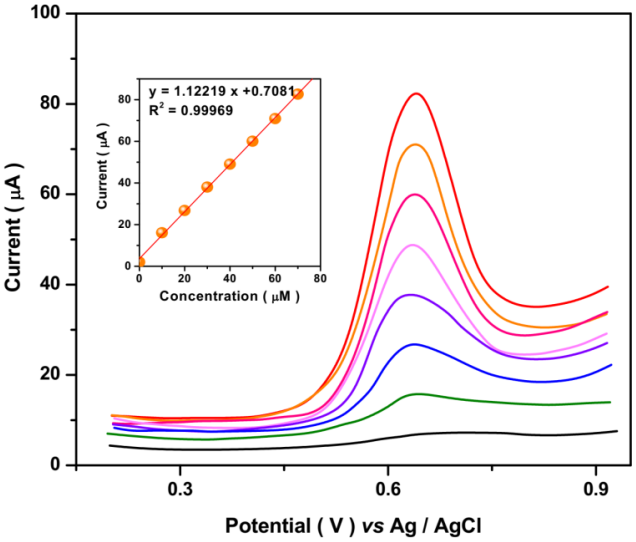

Figures 6. (a) The DPV curves of NiO@CNTs/GCE for successive injections of10µM fentanyl in 0.1M PBS pH 7.0at a scan rate of 20 mV/s; (b) the resulted calibration plot.

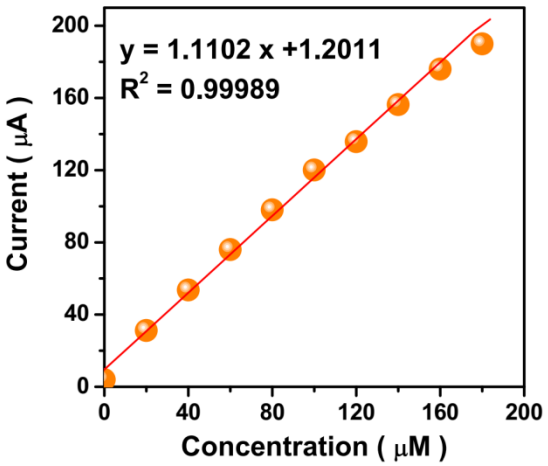

Figures 7. The resulted calibration plot of NiO@CNTs/GCE for successive injections of 20µM fentanyl in 0.1M PBS pH 7.0 at a scan rate of 20 mV/s

Moreover, the obtained sensing results of NiO@CNTs/GCE are compared with reported fentanyl electrochemical sensor in Table 1 which evidence to comparable or better sensing properties of NiO@CNTs/GCE than other reported electrochemical sensors. Furthermore, the wider linear range of the sensor in this study can be correlated with the high porosity and high effective surface of nanocomposites and synergistic effect of NiO nanoparticles and functionalized CNTs [36, 37].

Table 1. Comparison between the the obtained sensing results of NiO@CNTs/GCE with reported fentanyl electrochemical sensor.

Electrodes	**Technique**	**Detection limit (μM)**	**Linear range (μM)**	**Ref.**
NiO@CNTs/GCE	DPV	0.01	1–160	This work
Zn(II)- based metal-organic framework /Screen-printed electrode	DPV	0.3	1–100	[38]
Carbon nanoonions/GCE	DPV	0.3	1 – 60	[15]
MWCNT-polyethylenimine composite/flexible screen-printed carbon electrode	SWV [a]	10	10 – 100	[39]
Ionic Liquid/Screen-printed electrode	SWV	5	29.72–148.6	[40]
Screen-printed electrode	SWAdSV[b]	0.11	0.226–20.56	[41]
MWCNTs/GCE	CA[c]	0.1	0.5–100	[42]

[a]Square wave voltammetry;[b]Square-wave adsorptive stripping voltammetry; [c]Chronoamperometry

Table 2 also shows the results of the study of interference effect of main metabolites and organic compounds and drugs in body fluids such as ascorbic acid, oxycodone, uric acid, paracetamol, xanthine, albumin, hypoxanthine, glucose, zolpidem, nitrite and dopamine on determination of fentanyl using NiO@CNTs/GCE through the DPV experiments in 0.1 M PBS pH 7.0 at a scan rate of 20 mV/s. It is found in Table 2 that the NiO@CNTs/GCE demonstrates the significant electrocatalytic response to the addition of 1μM fentanyl, and addition of 10 μM of other interferant solutions do not show any remarkable response. Thus, the interferant in Table 2 do not interfere with the determination of fentanyl and the NiO@CNTs/GCE can be employed as a selective fentanyl sensor for analysis biological samples.

Table 2. The electrocatalytic response of DPV experiments of NiO@CNTs/GCE in 0.1M PBS pH 7.0 at scan rate of 20mV/s to addition of 1μM fentanyl, and addition of 10μM of other interferant solutions.

substance	**Added (μM)**	**Electrocatalytic response (μA) at** 0.64 V	**RSD* (%)**
fentanyl	1	1.1191	±0.0305
Ascorbic acid	10	0.0617	±0.0080
Oxycodone	10	0.0109	±0.0044
Uric acid	10	0.0177	±0.0043

Paracetamol	10	0.0512	±0.0039
Xanthine	10	0.0802	±0.0102
Albumin	10	0.0224	±0.0045
Hypoxanthine	10	0.0142	±0.0038
Glucose	10	0.0173	±0.0071
Zolpidem	10	0.0417	±0.0058
Nitrite	10	0.0113	±0.0051
Dopamine	10	0.0113	±0.0042

*Relative standard deviation

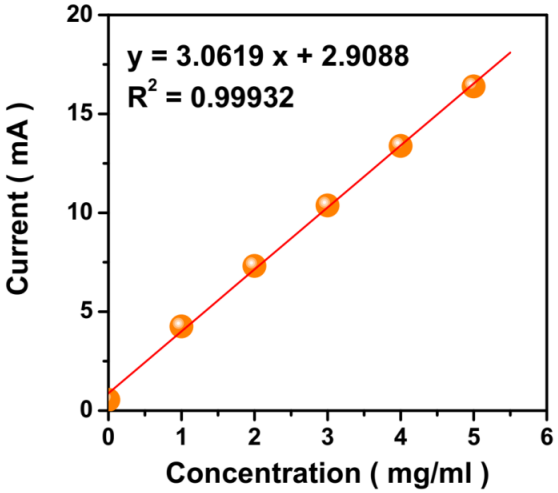

Figure 8. The obtained calibration plot of DPV responses of NiO@CNTs/GCE for determination of the fentanyl content in the prepared real sample of effentora tablet in successive additions of 1mg/ml fentanyl solution measurement in 0.1M PBS pH 7.0 at scan rate of 20mV/s

Table 3. Analytical results of standard addition method for analysis of both of fentanyl pharmaceutical and human serum samples

Sample	**Added (mg/ml)**	**Found (mg/ml)**	**Recovery (%)**	**RSD (%)**
Effentora tablets	0.00	0.95	-	-
	1.00	1.93	98.00	3.41
	2.00	2.91	98.00	3.22
	3.00	3.88	97.66	4.17
	4.00	4.85	97.50	3.09
	5.00	5.92	99.40	3.19
Human serum	0.00	0.00	-	-
	1.00	0.96	96.00	2.88
	2.00	1.94	97.00	3.15
	3.00	2.90	96.66	3.47
	4.00	3.89	97.25	4.21
	5.00	4.87	97.40	4.05

The performance and precision of the prepared electrodes were investigated for the analysis of fentanyl pharmaceutical and human serum samples using DPV measurement in 0.1M PBS pH 7 at a scan rate of 20mV/s with the standard addition method. Figure 8 displays the obtained calibration plot of DPV responses of NiO@CNTs/GCE for determination the fentanyl content in a prepared real sample of effentora tablet in successive additions of 1mg/ml fentanyl solution, demonstrating the fentanyl content in prepared pharmaceutical sample is 0.95 mg/ml which is very close to fentanyl concentration solution of tablets (1mg/ml). Furthermore, Table 3 shows the analytical results of standard addition method for analysis of both fentanyl pharmaceutical and human serum samples which implied acceptable precisions for analyses of real samples with good recovery values from96 to 99.40%and appropriate RSD values from 2.88 to 4.21%. Therefore, of NiO@CNTs/GCE can be applied to accurate and reliable determination of fentanyl in clinical analyses.

4. CONCULUSION

This study presented the synthesis of NiO@CNTs nanocomposite for modification of GCE and application for electrochemical determination of fentanyl. For modification of the GCE, the CNTs were functionalized under acid treatment, and then the functionalized CNTs and NiO was simultaneously electrodeposited on GCE. Results of structural showed that the surface of the 3D of CNTs network was homogeneously covered by NiO nanoparticles, and the simultaneous electrodeposition of NiO nanoparticles and functionalized CNTs on GCE had been created a core-shell structure of NiO and CNTs with large void space between neighboring nanostructures which can be beneficial for fast charge transfer in electrochemical reactions and easy access to electrolyte ions. The results of electrochemical studied exhibited that the good conductivity of NiO and CNTs can contribute to the enhancement of the electrochemical response of the electrode toward fentanyl. The NiO@CNTs/GCE showed the selective and stability to determination fentanyl, and sensitivity, limit of detection and linear range of NiO@CNTs/GCE as fentanyl sensor were obtained 1.12219 μA/μM, 0.01 μM and 10 to 160 μM, respectively. Moreover, a comparison between the obtained sensing results of NiO@CNTs/GCE with reported fentanyl electrochemical sensor demonstrated to comparable or better sensing properties and wider linear range of NiO@CNTs/GCE than other reported electrochemical sensors. The performance and precision of prepared electrodes were investigated for the analysis of fentanyl pharmaceutical and human serum samples and results indicated acceptable precisions for analyses of real samples with good recovery and appropriate RSD values. Therefore, the NiO@CNTs/GCE can be applied to accurate and reliable determination of fentanyl in clinical analyses.

ACKNOWLEDGEMENT
The research is supported by: Hubei Provincial Department of Education scientific research program guiding project, (No. B2016379).

References

1. S.D. Comer and C.M. Cahill, *Neuroscience & Biobehavioral Reviews*, 106 (2019) 49.
2. Y. Orooji, B. Tanhaei, A. Ayati, S.H. Tabrizi, M. Alizadeh, F.F. Bamoharram, F. Karimi, S. Salmanpour, J. Rouhi and S. Afshar, *Chemosphere*, 281 (2021) 130795.
3. M. Spetea, M. Faheem Asim, G. Wolber and H. Schmidhammer, *Current Pharmaceutical Design*, 19 (2013) 7415.
4. R. Mohamed, J. Rouhi, M.F. Malek and A.S. Ismail, *International Journal of Electrochemical Science*, 11 (2016) 2197.
5. Q. Zou, P. Xing, L. Wei and B. Liu, *Rna*, 25 (2019) 205.
6. H. Karimi-Maleh, Y. Orooji, F. Karimi, M. Alizadeh, M. Baghayeri, J. Rouhi, S. Tajik, H. Beitollahi, S. Agarwal and V.K. Gupta, *Biosensors and Bioelectronics*, 184 (2021) 113252.
7. X. Wang, Z. Feng, B. Xiao, J. Zhao, H. Ma, Y. Tian, H. Pang and L. Tan, *Green Chemistry*, 22 (2020) 6157.
8. H. Karimi-Maleh, M.L. Yola, N. Atar, Y. Orooji, F. Karimi, P.S. Kumar, J. Rouhi and M. Baghayeri, *Journal of colloid and interface science*, 592 (2021) 174.
9. C.A. Wong, B. Scavone, J. Slavenas, M. Vidovich, A. Peaceman, J. Ganchiff, T. Strauss-Hoder and R. McCarthy, *International journal of obstetric anesthesia*, 13 (2004) 19.
10. M. Niu, Y. Lin and Q. Zou, *Plant Molecular Biology*, 105 (2021) 483.
11. S. Sun, L. Xu, Q. Zou and G. Wang, *Bioinformatics*, 37 (2021) 1319.
12. H. Karimi-Maleh, S. Ranjbari, B. Tanhaei, A. Ayati, Y. Orooji, M. Alizadeh, F. Karimi, S. Salmanpour, J. Rouhi and M. Sillanpää, *Environmental Research*, 195 (2021) 110809.
13. X. Zhang, X. Sun, T. Lv, L. Weng, M. Chi, J. Shi and S. Zhang, *Journal of Materials Science: Materials in Electronics*, 31 (2020) 13344.
14. J. Rouhi, S. Mahmud, S.D. Hutagalung and N. Naderi, *Electronics letters*, 48 (2012) 712.
15. E. Sohouli, A.H. Keihan, F. Shahdost-fard, E. Naghian, M.E. Plonska-Brzezinska, M. Rahimi-Nasrabadi and F. Ahmadi, *Materials Science and Engineering: C*, 110 (2020) 110684.
16. M.W. Glasscott, K.J. Vannoy, P.A.I. Fernando, G.K. Kosgei, L.C. Moores and J.E. Dick, *TrAC Trends in Analytical Chemistry*, 132 (2020) 116037.
17. Z. He and H. Fan, *International Journal of Electrochemical Science*, 14 (2019) 9449.
18. H. Zhang and Y. He, *International Journal of Electrochemical Science*, 16 (2021) 210923.
19. L. Li, *International Journal of Electrochemical Science*, 16 (2021) 210917.
20. N. Naderi, M. Hashim, J. Rouhi and H. Mahmodi, *Materials science in semiconductor processing*, 16 (2013) 542.
21. S. Manzetti and J.-C.P. Gabriel, *International Nano Letters*, 9 (2019) 31.
22. N. Mohd Nurazzi, M. Muhammad Asyraf, A. Khalina, N. Abdullah, F.A. Sabaruddin, S.H. Kamarudin, S. Ahmad, A.M. Mahat, C.L. Lee and H. Aisyah, *Polymers*, 13 (2021) 1047.
23. P.M. Masipa, T. Magadzu and B. Mkhondo, *South African Journal of Chemistry*, 66 (2013) 173.
24. Z. Yu, L. Tetard, L. Zhai and J. Thomas, *Energy & Environmental Science*, 8 (2015) 702.
25. A. Saravanan, K. Prasad, N. Gokulakrishnan, R. Kalaivani and T. Somanathan, *Advanced Science, Engineering and Medicine*, 6 (2014) 809.
26. K. Luo, J. Zhang, W. Chu and H. Chen, *ACS omega*, 5 (2020) 24693.
27. H. Karimi-Maleh, Y. Orooji, A. Ayati, S. Qanbari, B. Tanhaei, F. Karimi, M. Alizadeh, J. Rouhi, L. Fu and M. Sillanpää, *Journal of Molecular Liquids*, 329 (2021) 115062.
28. R.A. Nuamah, S. Noormohammed and D.K. Sarkar, *Coatings*, 11 (2021) 780.
29. Z. Qiu, D. He, Y. Wang, X. Zhao, W. Zhao and H. Wu, *RSC advances*, 7 (2017) 7843.
30. C. Bittencourt, A. Felten, J. Ghijsen, J.-J. Pireaux, W. Drube, R. Erni and G. Van Tendeloo, *Chemical Physics Letters*, 436 (2007) 368.

31. M.W. Glasscott, K.J. Vannoy, P.A.I. Fernando, G.K. Kosgei, L.C. Moores and J.E. Dick, *TrAC Trends in Analytical Chemistry*, (2020) 116037.
32. M.R. Al-Bahrani, W. Ahmad, H.F. Mehnane, Y. Chen, Z. Cheng and Y. Gao, *Nano-micro letters*, 7 (2015) 298.
33. S. Zhang, X. Wang, Y. Li, X. Mu, Y. Zhang, J. Du, G. Liu, X. Hua, Y. Sheng and E. Xie, *Beilstein journal of nanotechnology*, 10 (2019) 1923.
34. H. Karimi-Maleh, M. Alizadeh, Y. Orooji, F. Karimi, M. Baghayeri, J. Rouhi, S. Tajik, H. Beitollahi, S. Agarwal and V.K. Gupta, *Industrial & Engineering Chemistry Research*, 60 (2021) 816.
35. L. Meng, C. Fu and Q. Lu, *Progress in Natural Science*, 19 (2009) 801.
36. Y. Cheng and P.K. Shen, *International journal of hydrogen energy*, 39 (2014) 20662.
37. D. Rajesh, P.I. Neel, A. Pandurangan and C. Mahendiran, *Applied Surface Science*, 442 (2018) 787.
38. E. Naghian, E.M. Khosrowshahi, E. Sohouli, F. Ahmadi, M. Rahimi-Nasrabadi and V. Safarifard, *New Journal of Chemistry*, 44 (2020) 9271.
39. A. Barfidokht, R.K. Mishra, R. Seenivasan, S. Liu, L.J. Hubble, J. Wang and D.A. Hall, *Sensors and Actuators B: Chemical*, 296 (2019) 126422.
40. S.A. Goodchild, L.J. Hubble, R.K. Mishra, Z. Li, K.Y. Goud, A. Barfidokht, R. Shah, K.S. Bagot, A.J. McIntosh and J. Wang, *Analytical chemistry*, 91 (2019) 3747.
41. C.E. Ott, H. Cunha-Silva, S.L. Kuberski, J.A. Cox, M.J. Arcos-Martínez and L.E. Arroyo-Mora, *Journal of Electroanalytical Chemistry*, 873 (2020) 114425.
42. N. Mostafa, E. Sohouli and F. Mousavi, *Journal of Analytical Chemistry*, 75 (2020) 1209.

© 2021 The Authors. Published by ESG (www.electrochemsci.org). This article is an open access article distributed under the terms and conditions of the Creative Commons Attribution license (http://creativecommons.org/licenses/by/4.0/).